



Transport and deposition of the fire biomarker levoglucosan across the tropical North Atlantic Ocean

Laura T. Schreuder^{a,*}, Ellen C. Hopmans^a, Jan-Berend W. Stuut^{b,c},
Jaap S. Sinninghe Damsté^{a,d}, Stefan Schouten^{a,d}

^a NIOZ Royal Netherlands Institute for Sea Research, Department of Marine Microbiology and Biogeochemistry, Utrecht University, P.O. Box 59, 1790 AB Den Burg, Texel, The Netherlands

^b NIOZ Royal Netherlands Institute for Sea Research, Department of Ocean Systems, Utrecht University, P.O. Box 59, 1790 AB Den Burg, Texel, The Netherlands

^c MARUM, Center for Marine Environmental Sciences, University of Bremen, Bremen, Germany

^d Department of Earth Sciences, Faculty of Geosciences, Utrecht University, P.O. Box 80.121, 3508 TA Utrecht, The Netherlands

Received 24 October 2017; accepted in revised form 10 February 2018; available online 21 February 2018

Abstract

Biomass burning impacts biogeochemical cycling, vegetation dynamics and climate. However, interactions between fire, climate and vegetation are not well understood and therefore studies have attempted to reconstruct fire and vegetation history under different climatic conditions using sedimentary archives. Here we focus on levoglucosan, a thermal by-product of cellulose generated during biomass burning, and, therefore, a potential fire biomarker in the marine sedimentary archive. However, before levoglucosan can be applied as a biomass burning proxy in marine sediments, there is a need for studies on how levoglucosan is transported to the marine environment, how it is reflecting biomass burning on continents, as well as the fate of levoglucosan in the marine water column and during deposition in marine sediments. Here we present analyses of levoglucosan, using an improved Ultra High Pressure Liquid Chromatography-Electro Spray Ionization/High Resolution Mass Spectrometry (UHPLC-ESI/HRMS) method, in atmospheric particles, in particulate matter settling through the water column and in marine surface sediments on a longitudinal transect crossing the tropical North Atlantic Ocean at 12°N. Levoglucosan was detected in the atmosphere, although in low concentration, possibly due to the sampled particle size, the source area of the aerosols, or the short time interval of sampling by which large burning events may have been missed. In sinking particles in the tropical North Atlantic Ocean we find that levoglucosan deposition is influenced by a mineral ballast effect associated with marine biogenic particles, and that levoglucosan is not transported in association with mineral dust particles. Highest levoglucosan concentrations and seasonal differences in sinking particles were found close to continents and low concentrations and seasonal differences were found in the open ocean. Close to Africa, levoglucosan concentration is higher during winter, reflecting seasonal burning in northwestern Africa. However, close to South America levoglucosan concentrations appear to be affected by riverine transport from the Amazon River. In surface sediments close to South America, levoglucosan concentration is higher than in the middle of the Atlantic Ocean, implying that here the influence from the South American continent is important and perennial. Our study provides evidence that degradation of levoglucosan during settling in the marine water column is not substantial, but is substantial at the sediment–water interface. Nevertheless, levoglucosan was detected in all surface sediments throughout the tropical North Atlantic, indicating its presence in the marine sedimentary record, which reveals the potential for levoglucosan as a biomass burning proxy in marine sediments.

© 2018 Elsevier Ltd. All rights reserved.

* Corresponding author.

E-mail address: laura.schreuder@nioz.nl (L.T. Schreuder).

1. INTRODUCTION

Fire has long been recognized to impact global ecosystem patterns and processes (Bond and Keeley, 2005) and it affects regional and global biogeochemical cycling, vegetation dynamics, climate, air quality and human health (e.g. Crutzen and Andreae, 1990; Bond and Keeley, 2005; Shakesby and Doerr, 2006; Bowman et al., 2009). Furthermore, wildfires in the last few decades have resulted in high economic costs in damages and subsequent health effects of smoke haze (e.g. Glover and Jessup, 2006). Nevertheless, large gaps remain in our understanding of the complex interactions between fire, climate and environment, despite an increasing need to manage fire and its emissions (Keywood et al., 2013), and integrate these interactions into Earth system models (Hantson et al., 2016). Therefore, fires have been studied at a wide range of temporal and spatial scales using satellites (e.g. Mouillot et al., 2014), historical data (e.g. Mouillot and Field, 2005) and dendrochronological data (e.g. Falk et al., 2011) for investigating the relation between climate, environment and fire, both at present as well as in the recent past.

Over longer (geological) time scales, sedimentary records have proven to be useful archives for proxies which enable the reconstruction of fire history (e.g. Daniau et al., 2013). Most of these studies use charcoal (e.g. Mooney and Tinner, 2011), black carbon (e.g. Han et al., 2016) or polycyclic aromatic hydrocarbons (e.g. Denis et al., 2012) as proxies for fire activity. However, application of these proxies in the sedimentary archive can sometimes be problematic. For example, there are many factors determining quantities of charcoal accumulating in lake sediments, such as lake and watershed size and the proportion of woody taxa (Hawthorne et al., *in press* and references therein), and also, this proxy mostly gives a rather local signal as the charcoal particles are only transported over relatively short distances. Polycyclic aromatic hydrocarbons are also formed during the combustion of other materials, such as fossil fuels (Peters et al., 2005), or during diagenesis of natural products (e.g. Koopmans et al., 1996) and are thus not specific enough as indicators for biomass burning. This illustrates that there is a need for additional biomass-burning proxies that cover a wider geographical area and have high source specificity.

A class of compounds commonly also associated with biomass burning are anhydrosugars, specifically levoglucosan (1,6-anhydro- β -D-glucose) and its isomers mannosan (1,6-anhydro- β -D-mannopyranose) and galactosan (1,6-anhydro- β -D-galactopyranose). These anhydrosugars are thermal products of cellulose/hemicelluloses formed at a temperature range of 150–350 °C (Shafizadeh et al., 1979; Simoneit et al., 1999; Kuo et al., 2011a). Levoglucosan is considered to be an ideal tracer for biomass burning in aerosols because of its high emission and source-specificity (e.g. Simoneit and Elias, 2000) and has been used in numerous air-quality studies (e.g. Iinuma et al., 2016). It has been shown that levoglucosan can degrade during long-range atmospheric transport by photo-oxidation (Zhao et al., 2014), heterogeneous reactions with OH radicals (Hennigan et al., 2010; Hoffmann et al., 2010; Kessler

et al., 2010; Teraji and Arakaki, 2010; Slade and Knopf, 2013, 2014; Lai et al., 2014) and NO₃ radicals (Knopf et al., 2011; Shiraiwa et al., 2012) and by multiphase oxidation by OH radicals (e.g. Arangio et al., 2015). However, it has been suggested that more direct atmospheric tracer studies are needed to further assess atmospheric degradation of levoglucosan (e.g. Myers-Pigg et al., 2016). Nevertheless, several studies have demonstrated that levoglucosan remains stable in the atmosphere for several days under most atmospheric conditions (Fraser and Lakshmanan, 2000; Mochida et al., 2003; Hu et al., 2013; García et al., 2017).

In contrast to aerosols, the use of levoglucosan and its isomers as a biomass burning proxy in geological archives is much more limited. To date, the analysis of levoglucosan in sedimentary archives has mostly focused on lake sediments (Elias et al., 2001; Sikes et al., 2013; Schüpbach et al., 2015; Shanahan et al., 2016; Battistel et al., 2017) and ice cores (Gambaro et al., 2008; Kawamura et al., 2012; Kehrwald et al., 2012; Zennaro et al., 2014; Seki et al., 2015; Wang et al., 2015; You et al., 2016). Only a few studies have analyzed this proxy in marine sediment cores (up to 130 ka), where it has shown its promise as a biomass burning proxy (Kuo et al., 2011b; Lopes dos Santos et al., 2013). Marine sediments have a high potential to reconstruct long-term (i.e. kyrs to myrs) variations in environmental and climate conditions and also cover a wide geographical region such as for example has been done with plant wax *n*-alkanes as a proxy for continental-scale vegetation (e.g. Bird et al., 1995; Huang et al., 2000; Schefuß et al., 2005; Castañeda et al., 2009; Schoon et al., 2015). Therefore, marine sediments may provide information on fire history on a regional to global scale, complementary to local to regional and global information from lake sediments and ice cores, respectively. Levoglucosan can be transported to marine sediments through the atmosphere and by rivers (Hunsinger et al., 2008). Furthermore, recent work confirms that levoglucosan is exported by particulate matter, although varying spatially and temporally, in rivers at a high enough level to potentially enter sedimentary deposits and record historical wildfire signatures (Myers-Pigg et al., 2017). However, before we can confidently apply levoglucosan as a biomass burning proxy in marine sediments, there is a need for studies on how levoglucosan is transported to the marine environment, how it is reflecting biomass burning on continents, as well as the fate of levoglucosan and its isomers while settling through the marine water column and during deposition in marine sediments.

Here we present analyses of levoglucosan and its isomers, using an improved Ultra High Pressure Liquid Chromatography-Electro Spray Ionization/High Resolution Mass Spectrometry (UHPLC-ESI/HRMS) method adapted from Hopmans et al. (2013), in atmospheric particles, in sinking marine particulate matter and in surface sediments collected along a longitudinal transect crossing the tropical North Atlantic Ocean at 12°N (Fig. 1). Particles emitted during biomass burning events in northwestern Africa have been shown to be transported along this transect (Freitas et al., 2005), making it suitable to trace the fate

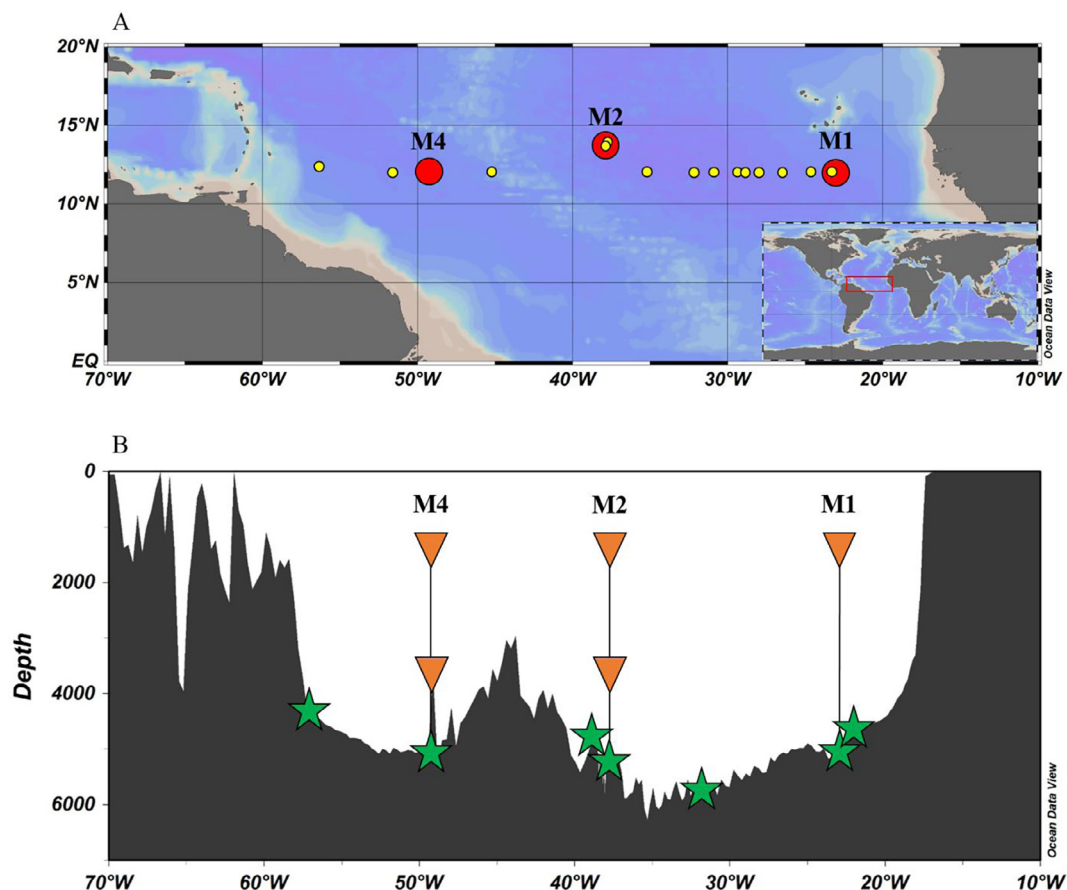


Fig. 1. (A) Longitudinal transect in the tropical North Atlantic Ocean at 12°N with the location of the sites for sediment trap deployment M1, M2 and M4 (red circles) and the location of aerosol sampling (yellow circles). The aerosol samples were either taken while sailing or while being stationary, and therefore the yellow circles represent either the middle of the sailed transect or the stationary location. In the bottom map (B) the location and depth of the sediment traps (orange triangles) and surface sediments (green stars) is shown in a bathymetry map along the transect. Both maps were generated in Ocean Data View. Figure adapted from Schreuder et al. (2018). (For interpretation of the references to colour in this figure legend, the reader is referred to the web version of this article.)

of biomass burning proxies. The sediment trap material has previously been studied for seasonal and spatial variations in long chain *n*-alkanes (Schreuder et al., 2018), in particle size of Saharan dust deposition (Van der Does et al., 2016), as well as for mass fluxes and their composition (Korte et al., 2017) and for coccolithophore fluxes (Guerreiro et al., 2017). Our results shed light on the longitudinal source-to-sink distribution and seasonal variability in levoglucosan deposition, and on depositional preservation of the levoglucosan signal in the tropical North Atlantic Ocean.

2. MATERIALS AND METHODS

2.1. Sample collection

Samples were collected in the tropical North Atlantic along a transect at 12°N (Fig. 1) as described previously (Schreuder et al., 2018). Briefly, 14 aerosol samples were collected using glass fiber filters while sailing the 12°N transect (Fig. 1) during cruise 64PE395 with the R/V *Pelagia*, between January 11 and February 6, 2015

(Stuut et al., 2015). The 11 aerosol samples collected between stations M1 and M2 were sampled during one multi-day dust event, while the three other samples were taken further west during another dust event. Sinking marine particulate matter was collected with five sediment traps along the same transect (Fig. 1). Three sediment traps were mounted to a cable at 1200 m water depth, at mooring stations M1, M2 and M4 (Fig. 1) and two sediment traps were mounted to a cable at 3500 m water depth, at mooring stations M2 and M4 (Fig. 1). All sediment traps were equipped with 24 sampling cups, collecting samples of sinking particulate matter at intervals of 16 days from October 2012 until November 2013 (for details see Stuut et al., 2012, 2013; Van der Does et al., 2016; Korte et al., 2017) and were retrieved during cruise 64PE378 with the R/V *Pelagia* between November 9 and December 6, 2013 (Stuut et al., 2013). In addition, surface sediments were collected with a multicorer at 7 stations (Fig. 1) during cruise M89 with the R/V *Meteor*, between October 3 and 25, 2012 (Stuut et al., 2012), as well as during cruise 64PE378 with the R/V *Pelagia* between November 9 and December 6, 2013 (Stuut et al., 2013).

2.2. Air-mass backward trajectories

In order to determine the provenance of the sampled atmospheric particles, six-day and eight-day backward trajectories of air parcels were calculated with the Hybrid Single Particle Lagrangian Integrated Trajectory (HYSPPLIT) model (Stein et al., 2015), using the GDAS (1.0°) meteorological dataset (<http://www.ready.noaa.gov/HYSPLIT.php>). Four aerosol sampling locations, spread over the transect at 12°N, were chosen and the starting points of the trajectories were at 23.26° W, 30.86° W, 42.21° W and 56.31° W. The height of the air layers were set to be 10 m and 100 m above ground level (AGL).

2.3. Analysis of levoglucosan and its isomers

2.3.1. Sample preparation for UHPLC-ESI/HRMS analysis

The 14 glass fiber filters used to collect aerosols were cut into small (~0.5 by 0.5 cm) pieces before extraction. The collected sinking particulate matter and the surface (0–1 cm) sediment was freeze-dried and homogenized. All samples were ultrasonically extracted (5×) with dichloromethane (DCM):methanol (MeOH) (2:1, v:v) and subsequently passed over a small Na₂SO₄ Pasteur pipette column with DCM. Deuterated (D7) levoglucosan (C₆H₃D₇O₅; dLVG, from Cambridge Isotope Laboratories, Inc.) was added in quantities ranging from 0.25 to 100 ng as an internal standard to quantify levoglucosan and its isomers mannosan and galactosan, after which they were dried under N₂. All extracts were re-dissolved in acetonitrile:H₂O (95:5, v:v) and filtered using a polytetrafluoroethylene (PTFE) filter (0.45 μm) before analysis.

2.3.2. UHPLC-ESI/HRMS analysis of levoglucosan and its isomers

We adapted the HPLC-ESI/MS² method of Hopmans et al. (2013) to a UHPLC-ESI/HRMS method using an Agilent 1290 Infinity UHPLC coupled to an Agilent 6230 Time-Of-Flight (TOF) mass spectrometer. Separation was achieved with two Acquity UPLC BEH amide columns (2.1 × 150 mm; 1.7 μm, Waters Chromatography) in series with a 50 mm guard column, which were kept at 30 °C. Compounds were eluted (0.2 ml min⁻¹) with 100% A (15 min), followed by back flushing with 100% B (15 min) and re-equilibration at starting conditions (25 min), resulting in a total analysis time of 55 min. Eluent A was a mixture of acetonitrile:H₂O (92.5:7.5, v:v) with 0.01% triethylamine (TEA) and eluent B was a mixture of acetonitrile:H₂O (70:30, v:v) with 0.01% TEA. Authentic standards for levoglucosan, galactosan and mannosan were all obtained from Sigma Aldrich. Conditions for negative ion Electrospray Ionization (ESI) were optimized by direct infusion of a levoglucosan solution into the source. Source settings were: nebulizer P 60 psi (N₂), VCap 5 kV and drying gas (N₂) 5 l/min at a temperature of 275 °C. The monitored mass range was *m/z* 150–350. Injection volume was usually 10 μl. Levoglucosan, its isomers, and dLVG were detected as their deprotonated molecules (M–H)⁻. Quantification was based on peak integrations of mass chromatograms within 3 ppm mass accuracy using a

calculated exact mass of 161.0445 *m/z* for levoglucosan (C₆H₁₀O₅) and its isomers and 168.0884 *m/z* (C₆H₃D₇O₅) for dLVG. Analytical performance and relative response factors (RRF) for levoglucosan, galactosan and mannosan compared to dLVG were determined by analysis of a standard mixture of levoglucosan, galactosan, mannosan and dLVG before and after analysis of samples and RRF varied between 1.03 and 1.20 for levoglucosan, between 0.33 and 0.64 for galactosan and between 0.75 and 0.94 for mannosan. Approximately 20% of the samples were analyzed in duplicate, which resulted in an average instrumental error of 5%.

3. RESULTS

3.1. Analytical method development for analysis of levoglucosan and its isomers

Levoglucosan and its isomers were analyzed using a UHPLC-ESI/HRMS method, adapted from the HPLC-ESI/MS² method of Hopmans et al. (2013), with deuterated levoglucosan (dLVG) as internal standard. We used two BEH amide columns in series, which resulted in improvement of separation of galactosan and mannosan to a chromatographic resolution of 1.0 and a retention time of 9.9 min for levoglucosan (Fig. 2). Response curves resulting from injections of 5 to 5000 pg on column for levoglucosan and its isomers showed a linear behavior with $R^2 > 0.99$ for all of them. The use of UHPLC/HRMS resulted in improved limit of quantitation as well as limit of detection for levoglucosan, i.e. 5 pg on column (S/N ~ 3).

3.2. Atmosphere

Levoglucosan was detected in all air filters, but mannosan or galactosan were not detected. The concentration of levoglucosan measured in air on the 12°N transect varies between 0.05 and 1.21 pg m⁻³ and shows highest values around 30°W and around 45–50°W (Fig. 3). In contrast, mineral dust (0.5–300 μm; Van der Does et al., 2016) concentrations along this transect vary between ~58 μg m⁻³ air close to the African continent and ~5 μg m⁻³ air in the samples furthest away from Africa and decrease with increasing distance from the coast (Schreuder et al., 2018) (Fig. 3).

Air-mass backward trajectories at four locations on the 12°N transect in the tropical North Atlantic ocean show that the air masses at the aerosol-sampling locations usually come from the northern and central parts of the Sahara region (Fig. 4B–D), or do not originate from the African continent (Fig. 4A).

3.3. Marine sinking particulate matter

Levoglucosan was detected in all sediment trap samples, but mannosan or galactosan were not detected. In marine sinking particles collected at 1200 m water depth, we find the highest average levoglucosan flux at location M1, closest to the African continent (2.9 ± 1.3 ng m⁻² d⁻¹), the lowest flux at location M2, in the open ocean (0.4 ± 0.2 ng

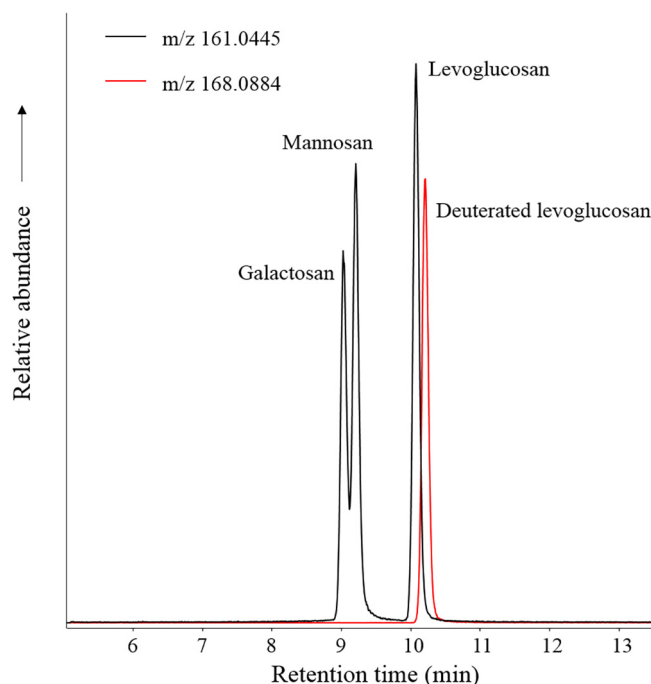


Fig. 2. UHPLC-ESI/HRMS mass chromatograms (3 ppm mass accuracy) showing levoglucosan, galactosan and mannosan (black line) and deuterated (D7) levoglucosan (red line) from a standard mixture (5 ng on column). (For interpretation of the references to colour in this figure legend, the reader is referred to the web version of this article.)

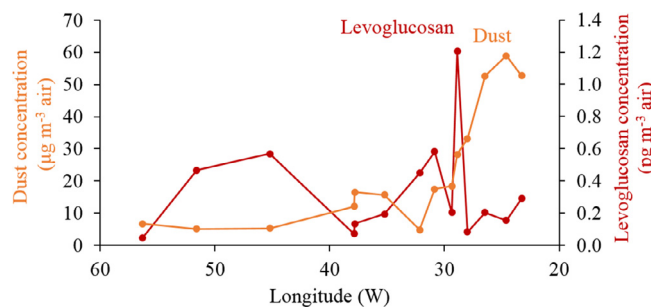


Fig. 3. Concentration of levoglucosan (red) and mineral dust in the air (orange) plotted against degrees longitude. (For interpretation of the references to colour in this figure legend, the reader is referred to the web version of this article.)

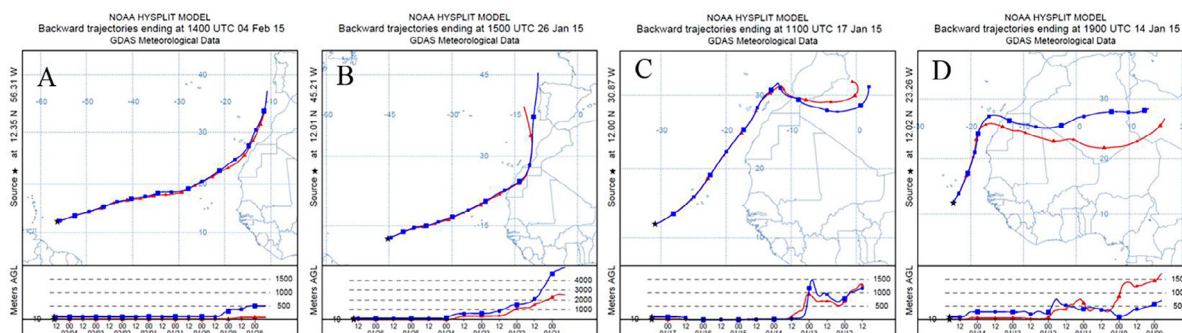


Fig. 4. Four eight-day (A) and six-day (B–D) air-mass backward trajectories of air parcels from aerosol-sampling locations at (A) 56.31° W, (B) 42.21° W, (C) 30.86° W and (D) 23.26° W, on the longitudinal transect at 12°N, at 10 m (red) and 100 m (blue) above ground level (AGL). These trajectories were calculated with the HYSPLIT model (<http://www.ready.noaa.gov/HYSPLIT.php>) and show trajectory maps (top) and elevation profiles (bottom). (For interpretation of the references to colour in this figure legend, the reader is referred to the web version of this article.)

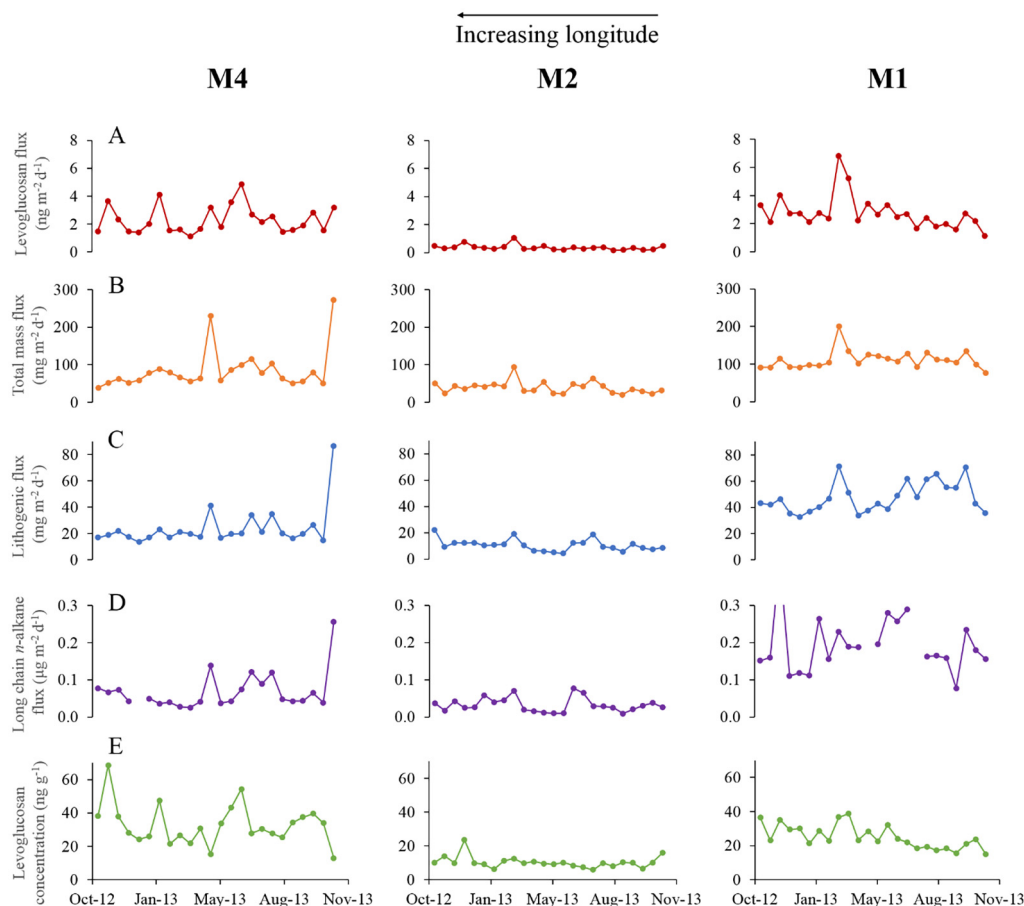


Fig. 5. Sediment trap time series from October 2012 until November 2013 at 1200 m water depth at locations M1, M2 and M4 of (A) levoglucosan flux, (B) total mass flux (from Korte et al., 2017), (C) lithogenic flux (from Korte et al., 2017), (D) long chain *n*-alkane flux (C_{25} – C_{33}), (E) levoglucosan concentration.

$m^{-2} d^{-1}$), and a higher flux again at location M4, closer to South America ($2.5 \pm 1.0 \text{ ng m}^{-2} d^{-1}$) (Fig. 5A). The concentration of levoglucosan in sinking particles shows a similar trend as the flux, with highest values close to continents and lower values at the open ocean, with flux-weighted average concentrations of 25.7 , 10.2 and 29.4 ng g^{-1} , at M1, M2 and M4, respectively (Fig. 5E). At location M1, closest to the African continent, there is a peak levoglucosan flux in February/March of 2013 (Fig. 5A), which is also visible in the levoglucosan concentration, although less pronounced (Fig. 5E). At the open ocean location M2 the levoglucosan peak flux in February/March is visible, but less pronounced than at location M1 (Fig. 5A), while the peak is not visible in the levoglucosan concentration (Fig. 5E). At the location close to South America (M4), levoglucosan flux and concentration are more variable throughout the year and show similar trends, with peaks in November and January, and higher values around June and September (Fig. 5A and E).

At location M2, the average levoglucosan flux in the lower sediment trap is higher ($0.6 \pm 0.2 \text{ ng m}^{-2} d^{-1}$) than

in the upper sediment traps ($0.4 \pm 0.2 \text{ ng m}^{-2} d^{-1}$) (Fig. 6A), while at location M4, the opposite trend is observed. Here, the average levoglucosan flux is lower in the lower sediment trap ($1.5 \pm 0.6 \text{ ng m}^{-2} d^{-1}$) compared to the upper sediment trap ($2.5 \pm 1.0 \text{ ng m}^{-2} d^{-1}$) (Fig. 6A). For the levoglucosan concentration in sinking particles we find similar values in the lower and upper sediment trap at both locations (Fig. 6E).

3.4. Surface sediments

Levoglucosan was detected in all surface sediments studied. Mannosan and galactosan were only present in trace amounts at location M1, and will not be discussed further. Levoglucosan concentrations vary between 0.19 and 1.52 ng g^{-1} sediment (Fig. 7). From 22°W to 49°W there is no clear trend in concentration with longitude. However, at the location closest to South America, the levoglucosan concentration is significantly ($p < 0.05$) higher at 1.52 ng g^{-1} sediment compared to surface sediment located more eastward (Fig. 7).

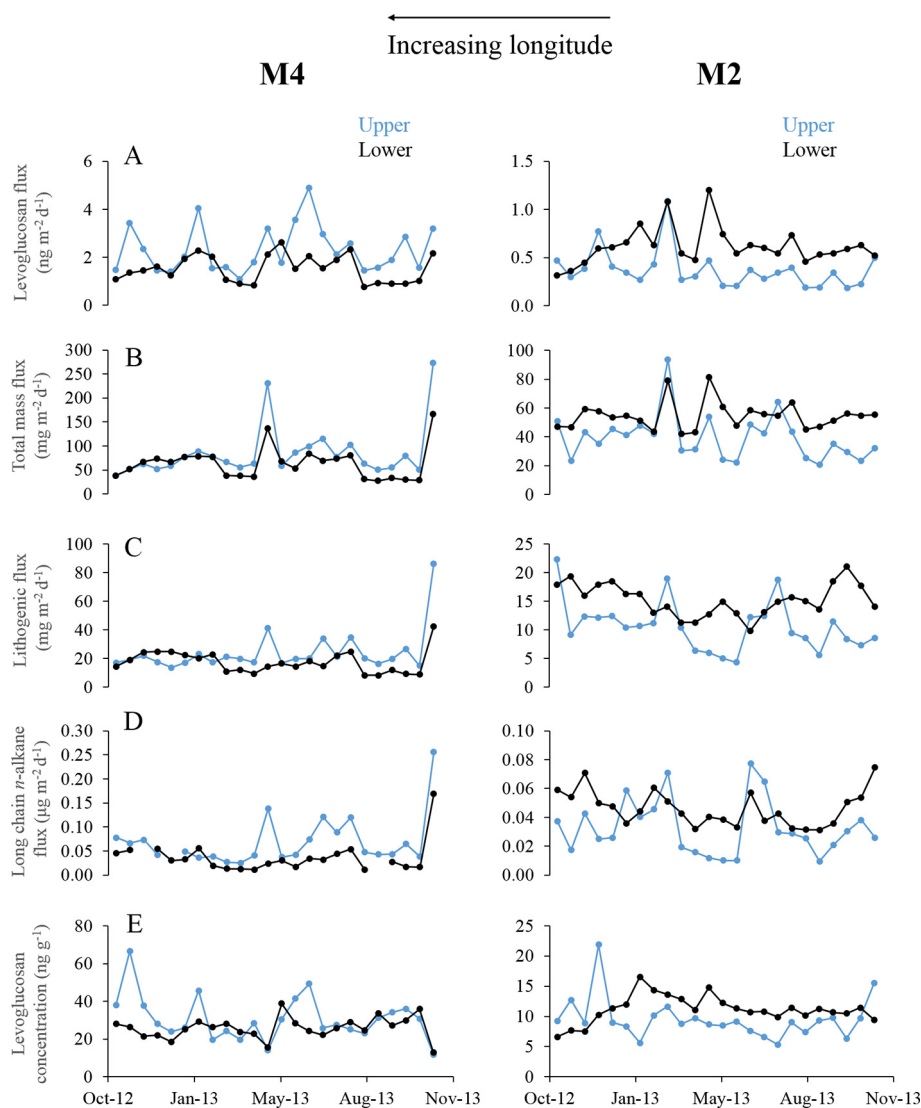


Fig. 6. Sediment trap time series from October 2012 until November 2013 at locations M2 and M4, at 1200 (blue) and 3500 m water depth (black) of the (A) levoglucosan flux, (B) total mass flux (from Korte et al., 2017), (C) lithogenic flux (from Korte et al., 2017), (D) long chain *n*-alkane flux (C_{25} – C_{33}) (from Schreuder et al., 2018), (E) levoglucosan concentration. (For interpretation of the references to colour in this figure legend, the reader is referred to the web version of this article.)

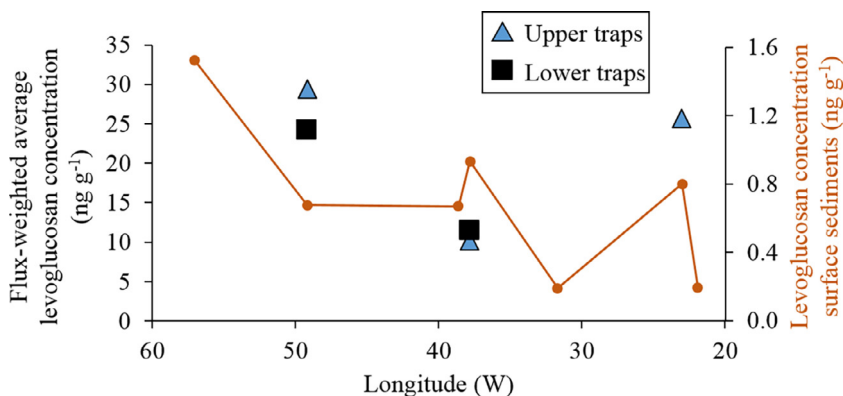


Fig. 7. The flux-weighted average levoglucosan concentration in the sinking particles at 1200 meters (blue triangles) and 3500 meters water depth (black squares), as well as levoglucosan concentrations in surface sediment (brown circles) along the 12°N transect in the North Atlantic Ocean. Note scale difference on y axes. (For interpretation of the references to colour in this figure legend, the reader is referred to the web version of this article.)

4. DISCUSSION

4.1. Improved analysis of levoglucosan and its isomers

The UHPLC-ESI/HRMS method is a substantial improvement over the HPLC-ESI/MS² method of Hopmans et al. (2013). Separation of galactosan and mannosan was improved compared to the HPLC-ESI/MS² method, where galactosan and mannosan co-eluted while here a resolution of 1.0 was obtained. Also, a larger retention time of 9.9 min for levoglucosan was obtained vs. 4.9 min for Hopmans et al. (2013), and is thus more distant from the injection peak making it more suitable for analysis of levoglucosan in samples with complex matrices. The use of UHPLC/HRMS improved the limit of quantitation as well as the limit of detection for levoglucosan, which was 5 pg on column (S/N ~ 3), and thus fivefold more sensitive than the original HPLC-ESI/MS² method (limit of detection 25 pg on column; Hopmans et al., 2013). Furthermore, dLVG was incorporated as an internal standard, which improves quantitation by allowing correction for matrix effects and machine performance.

4.2. Levoglucosan concentration in the atmosphere over the tropical North Atlantic

The concentration of levoglucosan in the atmosphere along the 12°N transect in the tropical North Atlantic Ocean, collected between January 11 and February 6 in the year 2015, is on average 0.33 pg m⁻³ air (Fig. 3), which is unusually low compared to other studies in remote oceanic locations. For example, Simoneit and Elias (2000) found levoglucosan concentrations ranging between 0.8 and 150 pg m⁻³ air collected at multiple oceanic locations around the world. Specifically for the North Atlantic Ocean, Puxbaum et al. (2007) sampled aerosols at the Azores over a two year period (July-2002 to July-2004) on a weekly basis and reported an average levoglucosan concentration of 6.6 ng m⁻³ air during the same season as in the current study (average over the months December, January and February), which is four orders of magnitude more than observed here. Fu et al. (2011) collected aerosols in December 1989 in the North Atlantic Ocean at around 30°N, further north than our transect at 12°N, and reported lower levoglucosan concentrations of 0.11 and 0.06 ng m⁻³ air, which are still two orders of magnitude higher than the concentrations reported here. The unusually low levoglucosan concentrations found in our study might be explained by the shorter sampling time of aerosols compared to other studies. We collected aerosols for ca. 10 h, which is considerably shorter than in the studies by Puxbaum et al. (2007) and Fu et al. (2011), who sampled for four or five days, respectively. Consequently, our short sampling time may have missed large burning events which resulted in large fluxes of levoglucosan. Furthermore, air-mass backward trajectories show that the air masses at the aerosol-sampling locations usually come from the northern and central parts of the Sahara region, or do not originate from the African continent (Fig. 4), while biomass burning takes place in the Sahel region which is located more southward

(e.g. Cooke et al., 1996). Therefore, it might be possible that the aerosols from biomass burning events in the Sahel did not reach the aerosol-sampling locations, which could be another explanation for the low levoglucosan concentration in the aerosols. Finally, the particle sizes analyzed have varied between studies. Similar to Fu et al. (2011) we used glass fiber filters with a diameter of about 0.4 μm, sampling all particles >0.4 μm. However, Puxbaum et al. (2007) studied the PM_{2.5} size fraction, i.e. particles with size <2.5 μm. The differences in size fraction analyzed could potentially lead to differences in levoglucosan concentration. Both laboratory and ambient measurements of smoke emissions from biomass burning processes have shown anhydrosugars to be predominantly present in the fine particle fraction <2.5 μm (e.g. Fine et al., 2004; Schkolnik et al., 2005; Engling et al., 2006; Herckes et al., 2006; Zhang et al., 2015). However, ambient measurements of smoke emissions collected in Texas, USA detected levoglucosan in larger aerosol particles with a diameter up to 10 μm (PM₁₀) (Fraser and Lakshmanan, 2000). Furthermore, Lee et al. (2008) found unusually high levoglucosan levels in PM₁₀ in rice-straw burning events and relate this to the ambient atmospheric conditions, such as high relative humidity and to unique properties of rice straw smoke and the specific burning practices of rice fields. This illustrates that levoglucosan is present in a wide range of aerosols particle sizes and that its abundance in the different aerosol particle fractions is depending on local conditions.

The highest levoglucosan concentrations were found around 30°W and around 45–50°W, and there is no decreasing trend with longitude (Fig. 3). This is in contrast with mineral dust concentrations as well as the plant wax long chain *n*-alkane, long chain *n*-alkanol and long chain fatty acid concentrations found on the same transect (Schreuder et al., 2018), which show a decreasing trend with increasing longitude. This decreasing trend in higher-plant biomarker concentrations with increasing distance from the African continent was explained by mineral dust settling from the atmosphere close to the source, as these biomarkers are transported predominantly with the mineral dust. The fact that levoglucosan does not correlate with downwind trends in the dust implies that levoglucosan is not predominantly transported with mineral dust particles.

4.3. Longitudinal and seasonal change in levoglucosan fluxes and concentrations in the tropical North Atlantic

4.3.1. Levoglucosan transport associated with particles in the marine water column

To evaluate if levoglucosan is transported to the tropical North Atlantic Ocean associated with mineral dust particles, the levoglucosan flux and lithogenic flux were correlated at each station at 1200 m water depth. It is assumed that the lithogenic flux reflects Saharan dust due to the similarity of lithogenic particles collected in the sediment traps and dust collected on the African coast (Korte et al., 2017) and the absence of major rivers transporting sediment to the study area. We find that there is no statistically significant correlation between the levoglucosan flux and the lithogenic flux at all three locations, i.e. location M1

(R^2 0.02 and $p = 0.502$), location M2 (R^2 0.03 and $p = 0.406$) and location M4 (R^2 0.14 and $p = 0.073$). The lack of correlation between the levoglucosan flux and the lithogenic flux thus confirms that levoglucosan is not transported together with Saharan dust. This supports a study by Falkovich et al. (2004), who found that levoglucosan is not adsorbed to mineral dust particles.

In contrast to the lithogenic flux, we do find a statistically significant correlation between the levoglucosan flux and total mass flux, at location M1 (R^2 0.66 and $p < 0.001$), location M2 (R^2 0.57 and $p < 0.001$), and also at location M4 (R^2 0.24 and $p = 0.014$). This implies that the deposition of levoglucosan is associated with settling of marine biogenic particles in the ocean, suggesting that levoglucosan is adsorbed to marine biogenic particles and transported to the sediment adsorbed to particulate matter, like has been observed for black carbon (Coppola et al., 2014). Indeed, levoglucosan deposited from the atmosphere is predominantly associated with fine-grained particles $< 2.5 \mu\text{m}$ (e.g. Fine et al., 2004) and therefore, like other labile organic matter, it will require mineral ballast in order to have sufficient density to settle down the water column. This is in contrast with long chain *n*-alkanes, which are associated with mineral dust particles (Schreuder et al., 2018), which probably act as a heavier ballast than the fine-grained particles with which levoglucosan is associated. Therefore, the fluxes of levoglucosan in the marine water column are likely mainly determined by total mass fluxes, i.e. biogenic particle productions, rather than the atmospheric particle fluxes.

4.3.2. Levoglucosan in sinking particles across the tropical North Atlantic

The highest levoglucosan flux in particles settling through the ocean at 1200 m water depth was found at location M1, close to the African continent (Fig. 5A), likely due to the fact that the highest total mass flux is also observed at this location (Fig. 5B; Korte et al., 2017). Interestingly, levoglucosan flux is highest during February/March, when total mass fluxes were also highest. However, it also coincides with the fire season in northwestern Africa, which is during the dry season, usually from November until February (e.g. Cooke et al., 1996). In fact, in the year of particle collection, fire intensity in northwestern Africa was highest during December, January and February (Fig. 8). To remove the impact of mineral ballast on the temporal pattern of levoglucosan, we plotted the concentration of levoglucosan in sinking particles rather than the levoglucosan flux (Fig. 5E). This also revealed highest concentrations in February/March, although less pronounced, and an overall higher concentration during winter compared to summer, implying that levoglucosan in sinking particles at 1200 m water depth also reflects the fire season in the northwestern part of the African continent. However, there seems to be a time lag of about one month between the fire season on the continent and the peak in levoglucosan concentration in the sinking particles at 1200 m water depth, which could be assigned to the transport time from source (continental fire) to sink (1200 m water depth, 800 km offshore Northwestern Africa). Dust-laden air usually

crosses the North Atlantic Ocean in about five to six days (Prospero, 1990), suggesting that the atmospheric transport of levoglucosan from the biomass burning plume to the surface waters at location M1 would take at most a few days. Korte et al. (2017) calculated a settling velocity of sinking particles of at least 140 m d^{-1} , which would result in a transport time to the sediment trap at 1200 m water depth of about 8–9 days. This would then result in a source-to-sink transport time of at least a couple of weeks, matching with the observed time lag.

The lowest levoglucosan flux and concentration in particles settling through the ocean was found at location M2, in the middle of the tropical North Atlantic Ocean (Fig. 5A and E). This agrees with the total mass flux, the lithogenic flux and the long chain *n*-alkane flux, which are also lowest at this open ocean location (Fig. 5B–D). The distinct levoglucosan peak in February/March detected at location M1 is also detected at location M2 in the levoglucosan flux (Fig. 5A), but not in the concentration (Fig. 5E), implying that at this location, the peak in levoglucosan flux is mainly caused by a mineral ballast effect associated with sinking particles in the water column. Overall, the levoglucosan concentration, as well as the total mass flux, the lithogenic flux and the long chain *n*-alkane flux were all found to be relatively invariable over the year at this location. The low values and seasonal variability in settling particles are expected here because of its remote location away from the continents, where the continental signal is likely to be more diluted and productivity is relatively low.

At location M4, close to the South American continent, levoglucosan concentration in marine sinking particles is higher than at location M1 and M2 (Fig. 5E), and shows a similar pattern as the levoglucosan flux (Fig. 5A). This indicates that here, the levoglucosan flux is not as strongly impacted by a mineral ballast effect as at location M2, which is also apparent from the lower correlation between levoglucosan flux and total mass flux at this location ($R^2 = 0.24$). Seasonal variability in levoglucosan concentration is higher than observed at location M2, but the seasonal peaks in concentration are at different times than at location M1 (Fig. 5E), i.e. in November and January, and also around June and September. This implies that levoglucosan emitted during seasonal burning in northwestern Africa is present only in minor amounts, and that there must be an additional source of levoglucosan in sinking particles at this location. Atmospheric transport of levoglucosan to location M4 could be derived from the South American continent, from the southern Amazon, where burning takes place during the dry season usually from July to October, or from the more northern parts of the continent, where biomass burning usually occurs from December to May (e.g. Duncan et al., 2003). In fact, in the year of particle collection, fire intensity in the southern part of South America was highest from August to October and in the northern parts of the continent burning was most intense from January to April (Fig. 8). However, the predominant wind direction across the tropical North Atlantic is from the east and biomass burning smoke from the southern Amazon is usually transported to the South Atlantic, to the Pacific Ocean and to the south of South America (Freitas et al.,

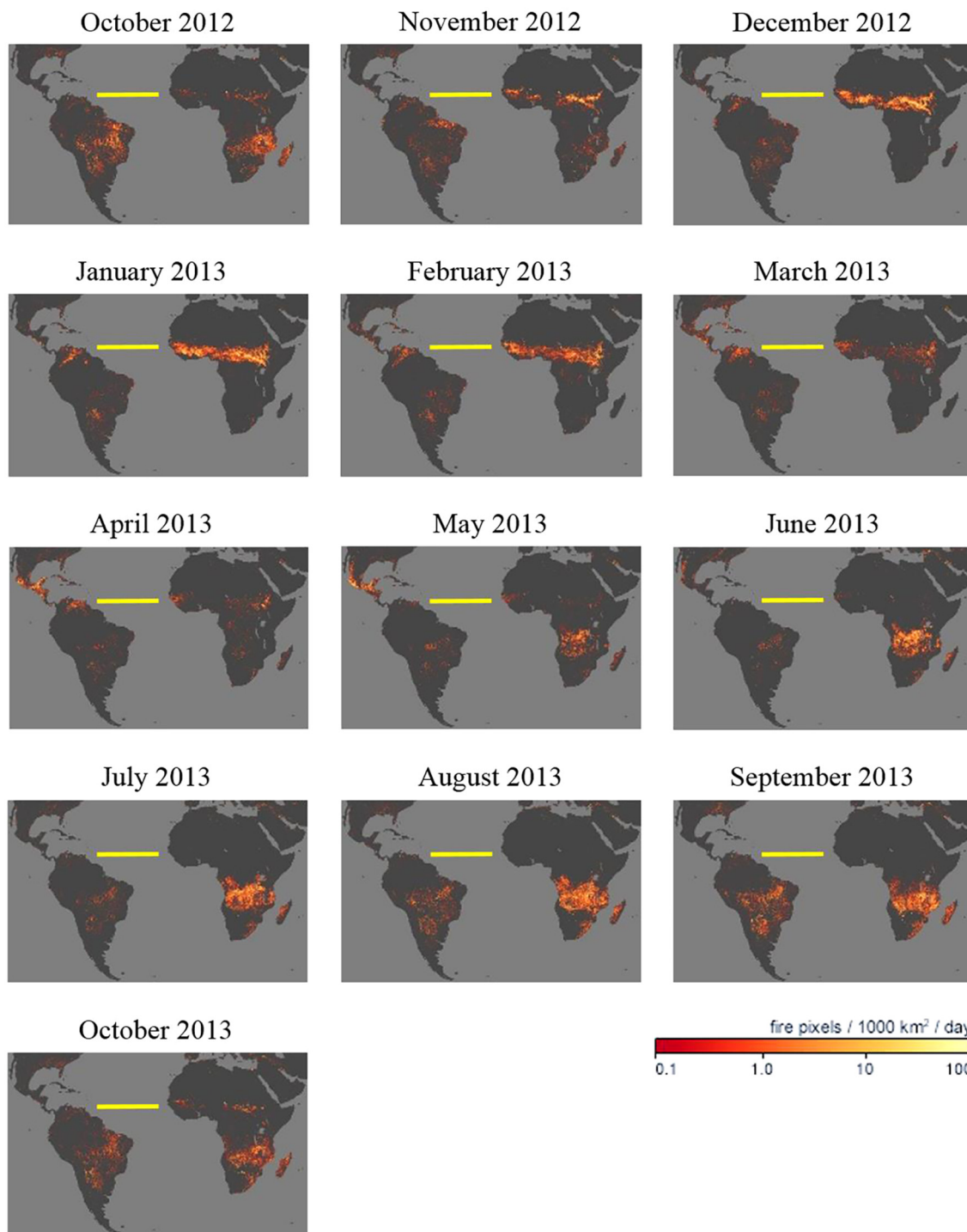


Fig. 8. Fire maps from October 2012 until October 2013, showing locations of actively burning fires around the world on a monthly basis, based on observations from the Moderate Resolution Imaging Spectroradiometer (MODIS) on NASA's Terra satellite. The colors are based on a count of the number of fires observed within a 1000-square-kilometer area, ranging from white (100 fires in a 1000-square-kilometer area per day) to red (1 fire per day). From https://earthobservatory.nasa.gov/GlobalMaps/view.php?d1=MOD14A1_M_FIRE. The yellow line represents the longitudinal transect at 12°N. (For interpretation of the references to colour in this figure legend, the reader is referred to the web version of this article.)

2005). It thus seems unlikely that atmospherically transported levoglucosan from the South American continent was present in the sinking particles at location M4,

although we cannot completely rule it out. However, it could also be that levoglucosan is transported with the Amazon River, which is discharging eastward towards

Africa between June and January (Muller-Karger et al., 1988). Indeed, an additional source in fluxes of long chain *n*-alkanes at location M4 coming from the Amazon River was already implied by Schreuder et al. (2018), although these fluxes were shown to be influenced by input from the Amazon River only during a peak in fall. Levoglucosan transport by the Amazon River is supported by recent studies, which have found that levoglucosan is transported to marine sediments by small mountainous rivers (Hunsinger et al., 2008) and, although varying spatially and temporally, that levoglucosan is exported by particulate matter in rivers at a high enough level to potentially enter sedimentary deposits (Myers-Pigg et al., 2017). Furthermore, pyrogenic organic matter export has previously been observed in rivers from the Amazon (e.g. Marques et al., 2017). Overall, the higher levoglucosan concentrations at both locations M1 and M4 confirms that closer to continents, we find higher levoglucosan concentrations and also more seasonal variability in levoglucosan input in sinking particles at 1200 m water depth in the tropical North Atlantic Ocean.

4.3.3. Levoglucosan in surface sediments across the tropical North Atlantic

The concentration of levoglucosan in surface sediments at location M1 is 0.80 ng g^{-1} (Fig. 7), which is higher than levoglucosan concentrations found in a marine sediment core in the Murray Canyon area, offshore southeast Australia, where an average concentration of 0.025 ng g^{-1} was reported and the most recent sediment (1.3 ka) had a levoglucosan concentration of 0.0003 ng g^{-1} (Lopes dos Santos et al., 2013). In sediment cores in two basins of the Puget Sound, offshore western USA, higher levoglucosan concentrations were found, ranging from 60 to 782 ng g^{-1} (Kuo et al., 2011b). However, the Puget Sound is a fjord-like estuary, and the sediment cores are thus located much closer to land than the marine sediments in the current study, which probably explains the much lower concentrations found in the tropical North Atlantic at location M1. At location M2 the levoglucosan concentration in the surface sediment is surprisingly comparable with the concentration found at location M1 (Fig. 7), implying that on a longer time-scale both locations receive the same amount of levoglucosan. This could be assigned to yearly variability in the amount of levoglucosan transported to the open ocean related to the extent and severity of biomass burning plumes on the continents, and that in the year of sampling the sinking particulate matter, levoglucosan was transported to this open ocean location in small amounts. Perhaps, more levoglucosan is transported as far as location M2 in other years, which could be possible as levoglucosan is usually associated with small particles that can be transported over large distances. At location M4, similar levoglucosan concentrations as at location M1 and M2 were found in the surface sediment (Fig. 7). This indicates that, while levoglucosan was transported to location M4 in higher amounts than to location M1 or M2 in the year of sampling the marine particulate matter in the sediment traps, this is not necessarily the case every year. However, in surface sediments located further west of location M4, closer to the South American coast, levoglucosan concen-

tration is significantly ($p < 0.05$) higher (Fig. 7). This implies that in the westernmost part of the transect, the additional input from South America is more important and perennial than at location M4. This is supported by the $\delta^{13}\text{C}$ values of higher plant-derived long chain *n*-alkanes, which indicated a significant contribution of C_3 -type vegetation such as from the Amazon rainforest, probably transported by the Amazon River (Schreuder et al., 2018).

4.4. Depositional preservation of levoglucosan

To investigate the preservation of levoglucosan in the tropical North Atlantic, while settling through the water column, levoglucosan fluxes in the upper (1200 m water depth) and lower (3500 m water depth) sediment traps at location M2 and M4 were compared (Fig. 6A). At location M2, the levoglucosan flux is higher in the lower trap compared to the upper trap (Fig. 6A), and the same is observed for the long chain *n*-alkane flux, total mass flux and lithogenic flux (Fig. 6B–D). This could be explained by the bigger catchment area for the lower trap compared to the upper trap (Siegel and Deuser, 1997; Waniek et al., 2000) as was also suggested by Korte et al. (2017) and Schreuder et al. (2018), resulting in higher input of particles in the lower trap compared to the upper trap. However, at location M4 we do not see this enrichment of particles in the lower trap. Instead, the levoglucosan flux is lower in the lower trap compared to the upper trap (Fig. 6A), as also observed in the long chain *n*-alkane flux, total mass flux and lithogenic flux (Fig. 6B–D). Schreuder et al. (2018) suggested that it could be that oceanic conditions, for example ocean currents, at this location are different from those at M2, leading to a different settling pathway of particles down the water column, and consequently, a different catchment area for the lower trap at location M4. Since we found that levoglucosan flux is mainly determined by total mass fluxes, we also compared levoglucosan concentrations in the upper and lower sediment traps at location M2 and M4 (Fig. 6E). At both locations, levoglucosan concentration is similar in the lower and the upper sediment traps, which implies that levoglucosan degradation in the water column is not substantial. This is in contrast with a study by Norwood et al. (2013), who have shown that levoglucosan is quickly degraded in water. Possibly, the adsorption of levoglucosan to marine biogenic particles has resulted in protection from biodegradation during transport through the marine water column, like has been observed for other labile materials when associated with minerals (e.g. Hedges et al., 1997). Therefore, it seems that adsorption of levoglucosan to biogenic particles is important for preservation of levoglucosan when transported through the water column.

To gain further insight into preservation of the levoglucosan signal during deposition in marine sediments, flux-weighted average levoglucosan concentrations in particles settling through the ocean were compared with those of surface sediments at the same locations (Fig. 7). The concentration of levoglucosan in the surface sediments is approximately two orders of magnitude lower than in the

particles settling through the water column (Fig. 7), indicating that whereas degradation apparently did not play a major role in the marine water column, degradation in marine sediments is substantial. This is in contrast with long chain *n*-alkanes, which do not show any substantial degradation in the same sediments (Schreuder et al., 2018). This is not unexpected as sugars are generally thought to be more labile than *n*-alkanes (e.g. Prahl et al., 1997) and the much longer time period of oxygen exposure in the surface sediment (decades to centuries) compared to the sediment traps is likely resulting in substantial degradation (Hartnett et al., 1998). Nevertheless, despite substantial degradation of levoglucosan in the surface sediments, it was detected at all stations, implying that levoglucosan can be traced back from the continent to deep open ocean sites and incorporated in the marine sedimentary archive.

To account for higher levoglucosan input into marine sediment associated with overall increased terrestrial input, and not necessarily associated with increased biomass burning activity on land, a ratio of levoglucosan and organic carbon has been used in aerosols (e.g. Puxbaum et al., 2007). Similarly, and more specific for terrestrial vegetation input, a ratio between long chain *n*-alkanes and levoglucosan could be used to account for increased terrestrial vegetation input into marine sediments. However, our results suggest that such a ratio is not useful, as differences in degradation rates as well as transport modes between the two components are large. Therefore, we hypothesize that in order to reconstruct past vegetation fires, absolute concentrations of levoglucosan should be used provided that preservational conditions did not change substantially. When preservational conditions change, e.g. by changes in oxic/anoxic conditions in the sediment, then the levoglucosan record could be biased. Also, changes in wind strength and direction could result in increased or decreased levoglucosan transport to the marine environment. Therefore, we suggest that in order to use levoglucosan as a biomass burning proxy in marine sediments on longer (geological) times scales, a multi-proxy study is needed to get a better understanding of the factors influencing the levoglucosan record.

5. CONCLUSIONS

Using an improved UHPLC-ESI/HRMS method, levoglucosan was detected in atmospheric particles, in particles settling through the ocean and in surface sediments along a longitudinal transect at 12°N in the tropical North Atlantic Ocean. Levoglucosan concentration in the atmosphere was unusually low, possibly due to the sampled particle size, the source area of the aerosols, or the short time interval of sampling. In sinking particles in the tropical North Atlantic Ocean we find that levoglucosan deposition is influenced by a mineral ballast effect associated with marine biogenic particles, and that levoglucosan is not transported in association with mineral dust particles. High levoglucosan concentrations in settling particles in the ocean at 1200 m water depth were found closest to the African continent (location M1), with highest concentration during February/March of 2013 and an overall higher con-

centration during winter, coinciding with the fire season in northwestern Africa. Lowest levoglucosan concentrations and seasonal variability in settling particles in the ocean at 1200 m water depth were found in the open ocean (location M2), where the continental signal is likely to be more diluted and productivity is relatively low. Closest to South America (location M4), levoglucosan concentration and seasonal variability in settling particles at 1200 m water depth is higher than at locations close to Africa. Moreover, in surface sediments further to the west, levoglucosan concentration is significantly higher than in surface sediments located more eastward. This implies that there is an additional source of levoglucosan from the South American continent, likely transported by the Amazon River. Our results provide evidence that degradation of levoglucosan in the water during settling in the water column is not substantial, possibly because of mineral protection. However, levoglucosan degradation is substantial at the sediment-water interface, probably related to the much longer time period of oxygen exposure in the surface sediment compared to the sediment traps. Nevertheless, levoglucosan was detected in all surface sediments throughout the tropical North Atlantic suggesting it can be incorporated in the marine sedimentary record.

ACKNOWLEDGEMENTS

We thank the captains and crews of R/V *Meteor* (cruise M89 in 2012) and R/V *Pelagia* (cruises 64PE378 in 2013 and 64PE395 in 2015) for deploying and collecting all the instruments that facilitated the sampling of the atmosphere, ocean and seafloor. M. van der Does and L.F. Korte are thanked for sampling and processing of the sediment trap samples. We thank three anonymous reviewers for their constructive comments which improved the manuscript. The research was funded by The Netherlands Organization for Scientific Research (NWO; project 824.14.001 and project 822.01.008, TRAFFIC) and by the European Research Council (ERC) project 311152, DUSTTRAFFIC. S.S. and J.S.S. D. are supported by the Netherlands Earth System Science Center (NESSC) funded by the Dutch Ministry of Science, Culture and Education.

APPENDIX A. SUPPLEMENTARY MATERIAL

Supplementary data associated with this article can be found, in the online version, at <https://doi.org/10.1016/j.gca.2018.02.020>.

REFERENCES

- Arangio A. M., Slade J. H., Berkemeier T., Pöschl U., Knopf D. A. and Shiraiwa M. (2015) Multiphase chemical kinetics of OH radical uptake by molecular organic markers of biomass burning aerosols: humidity and temperature dependence, surface reaction, and bulk diffusion. *J. Phys. Chem. A* **119**, 4533–4544.
- Battistel D., Argiriadis E., Kehrwald N., Spigariol M., Russell J. M. and Barbante C. (2017) Fire and human record at Lake Victoria, East Africa, during the Early Iron Age: did humans or climate cause massive ecosystem changes? *The Holocene* **27**, 997–1007.

- Bird M. I., Summons R. E., Gagan M. K., Roksandic Z., Dowling L., Head J., Fifield L. K., Cresswell R. G. and Johnson D. P. (1995) Terrestrial vegetation change inferred from n-alkane $\delta^{13}\text{C}$ analysis in the marine environment. *Geochim. Cosmochim. Acta* **59**, 2853–2857.
- Bond W. J. and Keeley J. E. (2005) Fire as a global ‘herbivore’: the ecology and evolution of flammable ecosystems. *Trends Ecol. Evol.* **20**, 387–394.
- Bowman D. M., Balch J. K., Artaxo P., Bond W. J., Carlson J. M., Cochrane M. A., D’Antonio C. M., DeFries R. S., Doyle J. C. and Harrison S. P. (2009) Fire in the Earth system. *Science* **324**, 481–484.
- Castañeda I. S., Mulitza S., Schefuß E., Lopes dos Santos R. A., Sinninghe Damsté J. S. and Schouten S. (2009) Wet phases in the Sahara/Sahel region and human migration patterns in North Africa. *Proc. Natl. Acad. Sci.* **106**, 20159–20163.
- Cooke W., Koffi B. and Gregoire J. M. (1996) Seasonality of vegetation fires in Africa from remote sensing data and application to a global chemistry model. *J. Geophys. Res.: Atmos.* **101**, 21051–21065.
- Coppola A. I., Ziolkowski L. A., Masiello C. A. and Druffel E. R. (2014) Aged black carbon in marine sediments and sinking particles. *Geophys. Res. Lett.* **41**, 2427–2433.
- Crutzen P. J. and Andreae M. O. (1990) Biomass burning in the tropics: Impact on atmospheric chemistry and biogeochemical cycles. *Science* **250**, 1669–1679.
- Daniau A.-L., Goñi M. F. S., Martinez P., Urrego D. H., Bout-Roumazelles V., Desprat S. and Marlon J. R. (2013) Orbital-scale climate forcing of grassland burning in southern Africa. *Proc. Natl. Acad. Sci.* **110**, 5069–5073.
- Denis E. H., Toney J. L., Tarozo R., Anderson R. S., Roach L. D. and Huang Y. (2012) Polycyclic aromatic hydrocarbons (PAHs) in lake sediments record historic fire events: validation using HPLC-fluorescence detection. *Org. Geochem.* **45**, 7–17.
- Duncan B. N., Martin R. V., Staudt A. C., Yevich R. and Logan J. A. (2003) Interannual and seasonal variability of biomass burning emissions constrained by satellite observations. *J. Geophys. Res.: Atmos.* **108**, 1–22.
- Elias V. O., Simoneit B. R., Cordeiro R. C. and Turcq B. (2001) Evaluating levoglucosan as an indicator of biomass burning in Carajas, Amazonia: a comparison to the charcoal record. *Geochim. Cosmochim. Acta* **65**, 267–272.
- Engling G., Carrico C. M., Kreidenweis S. M., Collett J. L., Day D. E., Malm W. C., Lincoln E., Hao W. M., Iinuma Y. and Herrmann H. (2006) Determination of levoglucosan in biomass combustion aerosol by high-performance anion-exchange chromatography with pulsed amperometric detection. *Atmos. Environ.* **40**, 299–311.
- Falk D. A., Heyerdahl E. K., Brown P. M., Farris C., Fulé P. Z., McKenzie D., Swetnam T. W., Taylor A. H. and Van Horn M. L. (2011) Multi-scale controls of historical forest-fire regimes: new insights from fire-scar networks. *Front. Ecol. Environ.* **9**, 446–454.
- Falkovich A. H., Schkolnik G., Ganor E. and Rudich Y. (2004) Adsorption of organic compounds pertinent to urban environments onto mineral dust particles. *J. Geophys. Res.: Atmos.* **109**, 1–19.
- Fine P. M., Chakrabarti B., Krudysz M., Schauer J. J. and Sioutas C. (2004) Diurnal variations of individual organic compound constituents of ultrafine and accumulation mode particulate matter in the Los Angeles basin. *Environ. Sci. Technol.* **38**, 1296–1304.
- Fraser M. P. and Lakshmanan K. (2000) Using levoglucosan as a molecular marker for the long-range transport of biomass combustion aerosols. *Environ. Sci. Technol.* **34**, 4560–4564.
- Freitas S. R., Longo K. M., Silva Dias M. A., Silva Dias P. L., Chatfield R., Prins E., Artaxo P., Grell G. A. and Recuero F. S. (2005) Monitoring the transport of biomass burning emissions in South America. *Environ. Fluid Mech.* **5**, 135–167.
- Fu P., Kawamura K. and Miura K. (2011) Molecular characterization of marine organic aerosols collected during a round-the-world cruise. *J. Geophys. Res.: Atmos.* **116**, 1–14.
- Gambaro A., Zangrando R., Gabrielli P., Barbante C. and Cescon P. (2008) Direct determination of levoglucosan at the picogram per milliliter level in Antarctic ice by high-performance liquid chromatography/electrospray ionization triple quadrupole mass spectrometry. *Anal. Chem.* **80**, 1649–1655.
- García M. I., Drooge B. L. v., Rodríguez S. and Alastuey A. (2017) Speciation of organic aerosols in the Saharan Air Layer and in the free troposphere westerlies. *Atmos. Chem. Phys.* **17**, 8939–8958.
- Glover D. and Jessup T. (2006) Indonesia’s fires and haze: the cost of catastrophe. IDRC.
- Guerreiro C. V., Baumann K.-H., Brummer G.-J. A., Fischer G., Korte L. F., Merkel U., Sa C., De Stigter H. and Stuu J. B. W. (2017) Coccolithophore fluxes in the open tropical North Atlantic: influence of the Amazon river and of Saharan dust deposition. *Biogeosciences* **14**, 1–22.
- Han Y., Peteet D., Arimoto R., Cao J., An Z., Sritrairat S. and Yan B. (2016) Climate and fuel controls on North American paleofires: smoldering to flaming in the late-glacial-holocene transition. *Sci. Reports* **6**, 20719.
- Hantson S., Kloster S., Coughlan M., Daniau A.-L., Vanniere B., Brücher T., Kehrwald N. and Magi B. I. (2016) Fire in the earth system: bridging data and modeling research. *Bull. Am. Meteorol. Soc.* **97**, 1069–1072.
- Hartnett H. E., Keil R. G., Hedges J. I. and Devol A. H. (1998) Influence of oxygen exposure time on organic carbon preservation in continental margin sediments. *Nature* **391**, 572, 572–572.
- Hawthorne D., Mustaphi C. J. C., Aleman J. C., Blarquez O., Colombaroli D., Daniau A.-L., Marlon J. R., Power M., Vannière B. and Han Y. (in press) Global Modern Charcoal Dataset (GMCD): a tool for exploring proxy-fire linkages and spatial patterns of biomass burning. *Quatern. Int.* <https://doi.org/10.1016/j.quaint.2017.1003.1046> (in press).
- Hedges J., Keil R. and Benner R. (1997) What happens to terrestrial organic matter in the ocean? *Org. Geochem.* **27**, 195–212.
- Hennigan C. J., Sullivan A. P., Collett J. L. and Robinson A. L. (2010) Levoglucosan stability in biomass burning particles exposed to hydroxyl radicals. *Geophys. Res. Lett.* **37**, 1–4.
- Herkes P., Engling G., Kreidenweis S. M. and Collett J. L. (2006) Particle size distributions of organic aerosol constituents during the 2002 Yosemite aerosol characterization study. *Environ. Sci. Technol.* **40**, 4554–4562.
- Hoffmann D., Tilgner A., Iinuma Y. and Herrmann H. (2010) Atmospheric stability of levoglucosan: a detailed laboratory and modeling study. *Environ. Sci. Technol.* **44**, 694–699.
- Hopmans E. C., dos Santos R. A. L., Mets A., Damsté J. S. S. and Schouten S. (2013) A novel method for the rapid analysis of levoglucosan in soils and sediments. *Org. Geochem.* **58**, 86–88.
- Hu Q.-H., Xie Z.-Q., Wang X.-M., Kang H. and Zhang P. (2013) Levoglucosan indicates high levels of biomass burning aerosols over oceans from the Arctic to Antarctic. *Sci. Reports* **3**, 3119.
- Huang Y., Dupont L., Sarnthein M., Hayes J. M. and Eglinton G. (2000) Mapping of C_4 plant input from North West Africa into North East Atlantic sediments. *Geochim. Cosmochim. Acta* **64**, 3505–3513.
- Hunsinger G. B., Mitra S., Warrick J. A. and Alexander C. R. (2008) Oceanic loading of wildfire-derived organic compounds

- from a small mountainous river. *J. Geophys. Res.: Biogeosci.* **113**, 1–14.
- Iinuma Y., Keywood M. and Herrmann H. (2016) Characterization of primary and secondary organic aerosols in Melbourne airshed: the influence of biogenic emissions, wood smoke and bushfires. *Atmos. Environ.* **130**, 54–63.
- Kawamura K., Izawa Y., Mochida M. and Shiraiwa T. (2012) Ice core records of biomass burning tracers (levoglucosan and dehydroabietic, vanillic and p-hydroxybenzoic acids) and total organic carbon for past 300 years in the Kamchatka Peninsula, Northeast Asia. *Geochim. Cosmochim. Acta* **99**, 317–329.
- Kehrwald N., Zangrando R., Gabrielli P., Jaffrezo J.-L., Boutron C., Barbante C. and Gambaro A. (2012) Levoglucosan as a specific marker of fire events in Greenland snow. *Tellus B* **64**, 18196.
- Kessler S. H., Smith J. D., Che D. L., Worsnop D. R., Wilson K. R. and Kröll J. H. (2010) Chemical sinks of organic aerosol: kinetics and products of the heterogeneous oxidation of erythritol and levoglucosan. *Environ. Sci. Technol.* **44**, 7005–7010.
- Keywood M., Kanakidou M., Stohl A., Dentener F., Grassi G., Meyer C., Torseth K., Edwards D., Thompson A. M. and Lohmann U. (2013) Fire in the air: biomass burning impacts in a changing climate. *Critical Rev. Environ. Sci. Technol.* **43**, 40–83.
- Knopf D. A., Forrester S. M. and Slade J. H. (2011) Heterogeneous oxidation kinetics of organic biomass burning aerosol surrogates by O₃, NO₂, N₂O₅, and NO₃. *Phys. Chem. Chem. Phys.* **13**, 21050–21062.
- Koopmans M. P., Köster J., Van Kaam-Peters H. M., Kenig F., Schouten S., Hartgers W. A., de Leeuw J. W. and Damsté J. S. S. (1996) Diagenetic and catagenetic products of isorenieratene: molecular indicators for photic zone anoxia. *Geochim. Cosmochim. Acta* **60**, 4467–4496.
- Korte L. F., Brummer G.-J. A., Van der Does M., Guerreiro C. V., Hennekam R., Hateren J. A. v., Jong D., Munday C. I., Schouten S. and Stuut J.-B. W. (2017) Downward particle fluxes of biogenic matter and Saharan dust across the equatorial North Atlantic. *Atmos. Chem. Phys.* **17**, 6023–6040.
- Kuo L.-J., Louchouart P. and Herbert B. E. (2011a) Influence of combustion conditions on yields of solvent-extractable anhydrosugars and lignin phenols in chars: Implications for characterizations of biomass combustion residues. *Chemosphere* **85**, 797–805.
- Kuo L.-J., Louchouart P., Herbert B. E., Brandenberger J. M., Wade T. L. and Creclius E. (2011b) Combustion-derived substances in deep basins of Puget Sound: historical inputs from fossil fuel and biomass combustion. *Environ. Pollut.* **159**, 983–990.
- Lai C., Liu Y., Ma J., Ma Q. and He H. (2014) Degradation kinetics of levoglucosan initiated by hydroxyl radical under different environmental conditions. *Atmos. Environ.* **91**, 32–39.
- Lee J. J., Engling G., Lung S. C. C. and Lee K. Y. (2008) Particle size characteristics of levoglucosan in ambient aerosols from rice straw burning. *Atmos. Environ.* **42**, 8300–8308.
- Lopes dos Santos R. A., De Deckker P., Hopmans E. C., Magee J. W., Mets A., Damsté J. S. S. and Schouten S. (2013) Abrupt vegetation change after the Late Quaternary megafaunal extinction in southeastern Australia. *Nat. Geosci.* **6**, 627–631.
- Marques J. S., Dittmar T., Niggemann J., Almeida M. G., Gomez-Saez G. V. and Rezende C. E. (2017) Dissolved black carbon in the headwaters-to-ocean continuum of Paraíba Do Sul River, Brazil. *Front. Earth Sci.* **5**.
- Mochida M., Kawamura K., Umemoto N., Kobayashi M., Matsunaga S., Lim H. J., Turpin B. J., Bates T. S. and Simoneit B. R. (2003) Spatial distributions of oxygenated organic compounds (dicarboxylic acids, fatty acids, and levoglucosan) in marine aerosols over the western Pacific and off the coast of East Asia: Continental outflow of organic aerosols during the ACE-Asia campaign. *J. Geophys. Res.: Atmos.* **108**, 1–12.
- Mooney S. and Tinner W. (2011) The analysis of charcoal in peat and organic sediments. *Mires and Peat* **7**, 1–18.
- Mouillot F. and Field C. B. (2005) Fire history and the global carbon budget: a 1×1 fire history reconstruction for the 20th century. *Global Change Biol.* **11**, 398–420.
- Mouillot F., Schultz M. G., Yue C., Cadule P., Tansey K., Ciais P. and Chuvieco E. (2014) Ten years of global burned area products from spaceborne remote sensing—a review: Analysis of user needs and recommendations for future developments. *Int. J. Appl. Earth Observ. Geoinform.* **26**, 64–79.
- Myers-Pigg A. N., Griffin R. J., Louchouart P., Norwood M. J., Sterne A. and Cevik B. K. (2016) Signatures of biomass burning aerosols in the plume of a saltmarsh wildfire in South Texas. *Environ. Sci. Technol.* **50**, 9308–9314.
- Myers-Pigg A. N., Louchouart P. and Teisserenc R. (2017) Flux of dissolved and particulate low-temperature pyrogenic carbon from two high-latitude rivers across the spring freshet hydrograph. *Front. Mar. Sci.* **4**, 38.
- Norwood M. J., Louchouart P., Kuo L.-J. and Harvey O. R. (2013) Characterization and biodegradation of water-soluble biomarkers and organic carbon extracted from low temperature chars. *Org. Geochem.* **56**, 111–119.
- Peters K. E., Walters C. C. and Moldowan J. M. (2005) *The Biomarker Guide*. Cambridge University Press.
- Prahl F. G., De Lange G. J., Scholten S. and Cowie G. L. (1997) A case of post-depositional aerobic degradation of terrestrial organic matter in turbidite deposits from the Madeira Abyssal Plain. *Org. Geochem.* **27**, 141–152.
- Prospero J. M. (1990) *Mineral-aerosol transport to the North Atlantic and North Pacific: The impact of African and Asian sources, The Long-Range Atmospheric Transport of Natural and Contaminant Substances*. Springer, Netherlands, pp. 59–86.
- Puxbaum H., Caseiro A., Sánchez-Ochoa A., Kasper-Giebl A., Claeys M., Gelencsér A., Legrand M., Preunkert S. and Pio C. (2007) Levoglucosan levels at background sites in Europe for assessing the impact of biomass combustion on the European aerosol background. *J. Geophys. Res.: Atmos.* **112**, 1–11.
- Schefuß E., Schouten S. and Schneider R. R. (2005) Climatic controls on central African hydrology during the past 20,000 years. *Nature* **437**, 1003–1006.
- Schkolnik G., Falkovich A. H., Rudich Y., Maenhaut W. and Artaxo P. (2005) New analytical method for the determination of levoglucosan, polyhydroxy compounds, and 2-methylerythritol and its application to smoke and rainwater samples. *Environ. Sci. Technol.* **39**, 2744–2752.
- Schoon P. L., Heilmann-Clausen C., Schultz B. P., Damsté J. S. S. and Schouten S. (2015) Warming and environmental changes in the eastern North Sea Basin during the Palaeocene-Eocene Thermal Maximum as revealed by biomarker lipids. *Org. Geochem.* **78**, 79–88.
- Schreuder L. T., Stuut J.-B. W., Korte L. F., Damsté J. S. S. and Schouten S. (2018) Aeolian transport and deposition of plant wax n-alkanes across the tropical North Atlantic Ocean. *Org. Geochem.* **115**, 113–123.
- Schüpbach S., Kirchgeorg T., Colombaroli D., Boffa G., Radaelli M., Kehrwald N. M. and Barbante C. (2015) Combining charcoal sediment and molecular markers to infer a Holocene fire history in the Maya Lowlands of Petén, Guatemala. *Quatern. Sci. Rev.* **115**, 123–131.

- Seki O., Kawamura K., Bendle J. A., Izawa Y., Suzuki I., Shiraiwa T. and Fujii Y. (2015) Carbonaceous aerosol tracers in ice-cores record multi-decadal climate oscillations. *Sci. Reports* **5**, 1–10.
- Shafizadeh F., Furneaux R. H., Cochran T. G., Scholl J. P. and Sakai Y. (1979) Production of levoglucosan and glucose from pyrolysis of cellulosic materials. *J. Appl. Polym. Sci.* **23**, 3525–3539.
- Shakesby R. and Doerr S. (2006) Wildfire as a hydrological and geomorphological agent. *Earth-Sci. Rev.* **74**, 269–307.
- Shanahan T. M., Hughen K. A., McKay N. P., Overpeck J. T., Scholz C. A., Gosling W. D., Miller C. S., Peck J. A., King J. W. and Heil C. W. (2016) CO₂ and fire influence tropical ecosystem stability in response to climate change. *Sci. Reports* **6**, 29587.
- Shiraiwa M., Pöschl U. and Knopf D. A. (2012) Multiphase chemical kinetics of NO₃ radicals reacting with organic aerosol components from biomass burning. *Environ. Sci. Technol.* **46**, 6630–6636.
- Siegel D. and Deuser W. (1997) Trajectories of sinking particles in the Sargasso Sea: modeling of statistical funnels above deep-ocean sediment traps. *Deep Sea Res. Part I: Oceanogr. Res. Papers* **44**, 1519–1541.
- Sikes E. L., Medeiros P. M., Augustinus P., Wilmshurst J. M. and Freeman K. R. (2013) Seasonal variations in aridity and temperature characterize changing climate during the last deglaciation in New Zealand. *Quatern. Sci. Rev.* **74**, 245–256.
- Simoneit B. R. and Elias V. O. (2000) Organic tracers from biomass burning in atmospheric particulate matter over the ocean. *Mar. Chem.* **69**, 301–312.
- Simoneit B. R., Schauer J. J., Nolte C., Oros D. R., Elias V. O., Fraser M., Rogge W. and Cass G. R. (1999) Levoglucosan, a tracer for cellulose in biomass burning and atmospheric particles. *Atmos. Environ.* **33**, 173–182.
- Slade J. H. and Knopf D. A. (2013) Heterogeneous OH oxidation of biomass burning organic aerosol surrogate compounds: assessment of volatilisation products and the role of OH concentration on the reactive uptake kinetics. *Phys. Chem. Chem. Phys.* **15**, 5898–5915.
- Slade J. H. and Knopf D. A. (2014) Multiphase OH oxidation kinetics of organic aerosol: The role of particle phase state and relative humidity. *Geophys. Res. Lett.* **41**, 5297–5306.
- Stein A., Draxler R. R., Rolph G. D., Stunder B. J., Cohen M. and Ngan F. (2015) NOAA's HYSPLIT atmospheric transport and dispersion modeling system. *Bull. Am. Meteorol. Soc.* **96**, 2059–2077.
- Stuut J. B., Boersen B., Bruck H. M., Hansen A., Koster B., Van der Does M. and Witte Y. (2012) Cruise Report RV Meteor M89, TRAFFIC I: Transatlantic Fluxes of Saharan Dust. 3–25 October 2012.
- Stuut J. B., Brummer G. J. A., Van der Does M., Friese C., Geerken E., van der Heide R., Korte L., Koster B., Metcalfe B., Munday C. I., van Ooijen J., Siccha M., Veldhuizen R., de Visser J.-D., Witte Y. and Wuis L. (2013) Cruise Report RV Pelagia 64PE378, TRAFFIC II: Transatlantic Fluxes of Saharan Dust. 9 November - 6 December 2013.
- Stuut J. B., Witte Y., de Visser J.-D., Boersen B., Koster B., Bakker K., Laan P., Van der Does M., Korte L., Munday C. and van Hateren H. (2015) Cruise Report RV Pelagia 64PE395, TRAFFIC III: Transatlantic Fluxes of Saharan Dust. 11 January - 6 February 2015.
- Teraji T. and Arakaki T. (2010) Bimolecular rate constants between levoglucosan and hydroxyl radical: Effects of pH and temperature. *Chem. Lett.* **39**, 900–901.
- Van der Does M., Korte L. F., Munday C. I., Brummer G.-J. A. and Stuut J.-B. W. (2016) Particle size traces modern Saharan dust transport and deposition across the equatorial North Atlantic. *Atmos. Chem. Phys.* **16**, 13697–13710.
- Wang M., Xu B., Kaspari S. D., Gleixner G., Schwab V. F., Zhao H., Wang H. and Yao P. (2015) Century-long record of black carbon in an ice core from the Eastern Pamirs: estimated contributions from biomass burning. *Atmos. Environ.* **115**, 79–88.
- Waniek J., Koeve W. and Prien R. D. (2000) Trajectories of sinking particles and the catchment areas above sediment traps in the northeast Atlantic. *J. Mar. Res.* **58**, 983–1006.
- You C., Xu C., Xu B., Zhao H. and Song L. (2016) Levoglucosan evidence for biomass burning records over Tibetan glaciers. *Environ. Pollut.* **216**, 173–181.
- Zennaro P., Kehrwald N., McConnell J. R., Schüpbach S., Maselli O. J., Marlon J., Vallelonga P., Leuenberger D., Zangrando R. and Spolaor A. (2014) Fire in ice: two millennia of boreal forest fire history from the Greenland NEEM ice core. *Clim. Past* **10**, 1905–1924.
- Zhang Z., Gao J., Engling G., Tao J., Chai F., Zhang L., Zhang R., Sang X., Chan C.-Y. and Lin Z. (2015) Characteristics and applications of size-segregated biomass burning tracers in China's Pearl River Delta region. *Atmos. Environ.* **102**, 290–301.
- Zhao R., Mungall E. L., Lee A. K., Aljawhary D. and Abbatt J. P. (2014) Aqueous-phase photooxidation of levoglucosan—a mechanistic study using aerosol time-of-flight chemical ionization mass spectrometry (Aerosol ToF-CIMS). *Atmos. Chem. Phys.* **14**, 9695–9706.

Associate Editor: Sarah J. Feakins